Study of the Effects of Parasitic Capacitance on Large Integrated Feedback Resistors for Charge-Sensitive Preamplifiers

S. Capra, A. Pullia

***Abstract*–A study of the impedance and noise of an integrated poly-silicon resistor with distributed capacitive coupling to bulk is presented. The system is analyzed by using a closed-form calculus which produces non approximated results. In particular, deviations from ideal conditions are shown when that kind of resistor is used as a continuous-discharge feedback device for charge-sensitive preamplifiers. The effect of using a feedback resistor with capacitive coupling to bulk is an evident deformation of the shape of the signals. An innovative technique is presented, which allows overcoming the problem of the distortions in the CSP output signals. Several n-wells are placed under the resistor and driven with an auxiliary low-impedance divider which minimizes the voltage variations on the plates of the parasitic capacitors. In this way the pulses provided by the charge-sensitive preamplifiers show again a clean R-C exponential-decay shape and are so optimized for signal shaping and adequate for high-resolution spectroscopy.**

I. Introduction

Charge sensitive preamplifiers generally use a physical resistor as a continuous–time reset device: higher resistance values correspond to lower current noise and better spectroscopic performances. In the process of integration of the CSP the realization of this feedback device is a non-trivial task. Generally for gamma-ray spectroscopy a feedback resistor is used in the GΩ range, but an integrated poly-silicon resistor of such value is critical in terms of area occupancy. The physical dimension is not the only issue: in fact the distributed capacitive coupling to bulk tends to turn such device into a distributed transmission line and a simple resistor model is no longer adequate. Here a study is carried out of the impedance and the noise of this distributed-parameter device and a solution is proposed to minimize the effects of the distributed capacitance. The device, realized in AMS 0.35μm, was connected as a feedback resistor to a charge-sensitive preamplifier realized with a commercial operational amplifier. The experimental data, which show the output signals of the CSP, demonstrate the validity of the solution proposed and ensure that the behavior of the real system is in agreement with the theoretical study.

Manuscript received November 30, 2014.

S. Capra is with the Department. of Physics, University of Milano, Milano, Italy (e-mail: Stefano.capra@unimi.it).

A. Pullia is with the Department. of Physics, University of Milano, Milano, Italy and INFN, Milano, Italy (e-mail: alberto.pullia@mi.infn.it).

II. Study of the Impedance

We study the impedance of the system considering at first a simple single R-C cell, as depicted in Fig. 1. Instead of writing the usual impedance matrix, we prefer to express the relations between voltages and currents in the following form.

$$\begin{pmatrix} V_0 \\ I_0 \end{pmatrix} = \begin{pmatrix} 1+sRC & R \\ sC & 1 \end{pmatrix} \begin{pmatrix} V_1 \\ I_1 \end{pmatrix} \qquad (1)$$

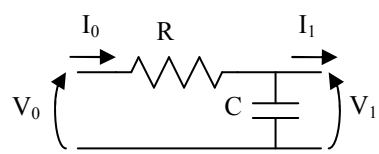

Fig. 1. Schematic diagram of the single R-C cell. Voltages and currents are explicitly indicated in order to match the notation of (1).

If we connect the output of a cell with the input of another one as in Fig. 2 and calculate the equations of the new system, we realize that they can be simply described with the matrix product of two single R-C cells.

$$\begin{pmatrix} V_0 \\ I_0 \end{pmatrix} = \begin{pmatrix} 1+sRC & R \\ sC & 1 \end{pmatrix} \begin{pmatrix} 1+sRC & R \\ sC & 1 \end{pmatrix} \begin{pmatrix} V_1 \\ I_1 \end{pmatrix} \qquad (2)$$

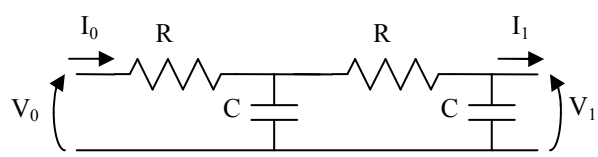

Fig. 2. Schematic diagram of a double R-C cell. Voltages and currents are explicitly indicated in order to match the notation of (2).

Starting from this simple consideration, we understand that we can connect together an arbitrary number of cells and obtain the correct equations by just writing the product of a number of R-C matrices. Now we can represent the physical device as a cascade connection of n such cells, as depicted in Fig. 3. The model approaches the real system in the limit for $n \to \infty$. We don't need to calculate again the impedance of this system respect to the number of cells. In fact, we just need to treat each R-C cell as an independent device, which is well described by (1). The behavior of such a composite system can

be correctly described using the n-th power of the matrix of the single cell (3). It's interesting to note that most simulators adopt a model of the resistance with distributed capacitive coupling to bulk just with a finite number of R-C cells.

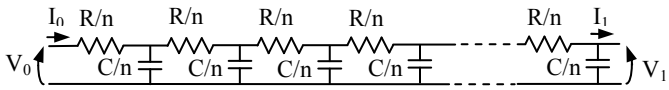

Fig. 3. Schematic diagram of a chain of n R-C cells. They represent a physical device with total resistance R and total capacitive coupling to bulk C. Dividing the system into n separate cells generates obviously a series of resistances of value R/n and C/n.

$$\begin{pmatrix} V_0 \\ I_0 \end{pmatrix} = \begin{pmatrix} 1 + s\frac{RC}{n^2} & \frac{R}{n} \\ s\frac{C}{n} & 1 \end{pmatrix}^n \begin{pmatrix} V_1 \\ I_1 \end{pmatrix} \tag{3}$$

Now we should remember that the power of a matrix can be easily calculated with a base change which turns the matrix into a diagonal one. To do so, let's calculate the eigenvalues and the eigenvectors. After straightforward calculations (3) can be rewritten in the following form:

$$\begin{pmatrix} V_0 \\ I_0 \end{pmatrix} = (B) \begin{pmatrix} {\lambda_1}^n & 0 \\ 0 & {\lambda_2}^n \end{pmatrix} (B^{-1}) \begin{pmatrix} V_1 \\ I_1 \end{pmatrix}, \tag{4}$$

where λ_1, λ_2, B and B^{-1},are equal to:

$$\lambda_{1,2} = \frac{\mp\sqrt{sRC(sRC+4\,n^2)}+sRC+2n^2}{2n^2}, \tag{5}$$

$$B = \begin{pmatrix} -\frac{R\sqrt{sC}+\sqrt{R(4n^2+sRC)}}{2n\sqrt{sC}} & -\frac{R\sqrt{sC}-\sqrt{R(4n^2+sRC)}}{2n\sqrt{sC}} \\ 1 & 1 \end{pmatrix} \tag{6}$$

and $$B^{-1} = \begin{pmatrix} -\frac{n\sqrt{sC}}{\sqrt{R(4n^2+sRC)}} & \frac{R\sqrt{sC}+\sqrt{R(4n^2+sRC)}}{2\sqrt{R(4n^2+sRC)}} \\ \frac{n\sqrt{sC}}{\sqrt{R(4n^2+sRC)}} & -\frac{R\sqrt{sC}-\sqrt{R(4n^2+sRC)}}{2\sqrt{R(4n^2+sRC)}} \end{pmatrix}. \tag{7}$$

In order to describe the resistance with distributed capacitance like the one in Fig. 4, we should switch from a discrete model to a continuous one. This can be accomplished by raising the number of cells to infinity. This can be done by calculating the limit for n→∞ for the central matrix and for B and B^{-1} separately. The result is the analytical expression for voltages and currents of the physical resistor with distributed coupling to bulk. In order to evaluate the limit for $n \to \infty$ we can calculate the limits for λ_1, λ_2, B and B^{-1} separately, thus obtaining (8).

$$\begin{pmatrix} V_0 \\ I_0 \end{pmatrix} = \begin{pmatrix} cosh\,(\sqrt{sRC}) & \sqrt{\frac{R}{sC}}senh(\sqrt{sRC}) \\ \sqrt{\frac{sC}{R}}senh(\sqrt{sRC}) & cosh(\sqrt{sRC}) \end{pmatrix} \begin{pmatrix} V_1 \\ I_1 \end{pmatrix} \tag{8}$$

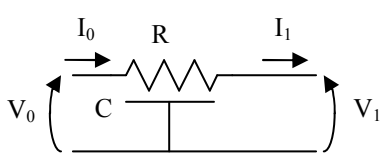

Fig. 4. Schematic diagram of the distributed-impedance resistor with capacitive coupling. Voltages and currents are explicitly indicated in order to match the notation of (8).

It is worth noting that both in the limit for $s \to 0$ and $C \to 0$ the matrix in (8) becomes equal to the one of a simple, ideal resistor (9), which guarantees the coherence of the method adopted.

$$\begin{pmatrix} V_0 \\ I_0 \end{pmatrix} = \begin{pmatrix} 1 & R \\ 0 & 1 \end{pmatrix} \begin{pmatrix} V_1 \\ I_1 \end{pmatrix} \tag{9}$$

III. Study of the Noise

Now with a similar procedure we can evaluate the current noise generated by such a device when connected as a feedback resistor of a CSP. We assume to short-circuit to ground both the terminals of the resistor and evaluate the current noise which flows through them. We should remember that in a CSP one terminal of the feedback resistor is connected to the low impedance output of the preamplifier and the other one to the virtual ground. We start from writing the equations which describe a single noisy R-C cell like the one in Fig. 5.

$$\begin{pmatrix} V_0 \\ I_0 \\ 1 \end{pmatrix} = \begin{pmatrix} 1 + \frac{sRC}{n^2} & \frac{R}{n} & 2\sqrt{\frac{kRT}{n}} \\ \frac{sC}{n} & 1 & 0 \\ 0 & 0 & 1 \end{pmatrix} \begin{pmatrix} V_1 \\ I_1 \\ 1 \end{pmatrix} \tag{10}$$

Notice that to introduce the thermal noise of the resistance we were forced to switch from a bidimensional formalism to a tridimensional one.

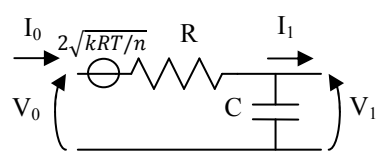

Fig. 5. Schematic diagram of a single noisy R-C cell. Voltages and currents are explicitly indicated in order to match the notation of (10).

We represent the real distributed-impedance device with a series of noisy R-C cells like the one in Fig. 6. The total power of current noise generated by the whole system can be obtained summing the contributions of all the n resistances which constitute the device. We write the usual matrix product to define the relations between voltages and currents (11).

$$\begin{pmatrix} V_0 \\ I_0 \\ 1 \end{pmatrix} = \begin{pmatrix} 1 + \frac{sRC}{n^2} & \frac{R}{n} & 0 \\ \frac{sC}{n} & 1 & 0 \\ 0 & 0 & 1 \end{pmatrix}^{n-m-1} \cdot \begin{pmatrix} 1 + \frac{sRC}{n^2} & \frac{R}{n} & 2\sqrt{\frac{kRT}{n}} \\ \frac{sC}{n} & 1 & 0 \\ 0 & 0 & 1 \end{pmatrix} \cdot \begin{pmatrix} 1 + \frac{sRC}{n^2} & \frac{R}{n} & 0 \\ \frac{sC}{n} & 1 & 0 \\ 0 & 0 & 1 \end{pmatrix}^m \cdot \begin{pmatrix} V_1 \\ I_1 \\ 1 \end{pmatrix} \tag{11}$$

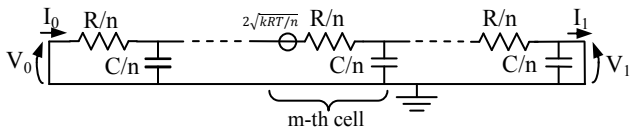

Fig. 6. Schematic diagram of the group of n R-C cells. Only the m-th one is noisy. Voltages and currents are explicitly indicated in order to match the notation of (11).

We can express (11) in the following form.

$$\begin{pmatrix} V_0 \\ I_0 \\ 1 \end{pmatrix} = M_{m,n} \begin{pmatrix} V_1 \\ I_1 \\ 1 \end{pmatrix} \tag{12}$$

Where

$$M_{m,n} = (B) \begin{pmatrix} {\lambda_1}^{n-m-1} & 0 & 0 \\ 0 & {\lambda_2}^{n-m-1} & 0 \\ 0 & 0 & 1 \end{pmatrix} (B^{-1}) \cdot$$

$$\cdot \begin{pmatrix} 1 + \frac{sRC}{n^2} & \frac{R}{n} & 2\sqrt{\frac{kRT}{n}} \\ \frac{sC}{n} & 1 & 0 \\ 0 & 0 & 1 \end{pmatrix} (B) \begin{pmatrix} {\lambda_1}^{m} & 0 & 0 \\ 0 & {\lambda_2}^{m} & 0 \\ 0 & 0 & 1 \end{pmatrix} (B^{-1}) \tag{13}$$

Now, solving (13) and rearranging the terms, we write a new matrix, which still depends on m and n but satisfies (14).

$$\begin{pmatrix} I_1 \\ I_0 \\ 1 \end{pmatrix} = M'_{m,n} \begin{pmatrix} V_1 \\ V_0 \\ 1 \end{pmatrix} \tag{14}$$

$|I_0|$ now represents the square root of the power of current noise flowing through the left terminal due to the contribution of the m-th cell. We must solve both the limit and the sum of (13) in order to find the total power of current noise generated at both terminals due to thermal noise.

$$i^2_{noise,0} = \lim_{n\to\infty} \sum_{m=0}^{n-1} \left(|\mathrm{I}_{0,m,n}|\right)^2$$

$$= i^2_{noise,1} = \lim_{n\to\infty} \sum_{m=0}^{n-1} \left(|\mathrm{I}_{1,m,n}|\right)^2 \tag{15}$$

This can be a tricky task, however there are different approaches to find a solution: the best one is to transform the sum into an integral and then solve the limit. It is also possible to write the two halves of the resistor on the left and on the right of the noisy cell in (13) like in (8) and then follow the same procedure. Generally the current noise produced is white for low frequencies, as in the ideal case, with a spectral density equal to the one of the classical model $4KT/R$, but for high frequencies it goes like the square root of frequency. The noise corner frequency depends both on R and C. The key idea is that the capacitive coupling at high frequencies tends to reduce the effective value of the device so that it starts to produce a higher current noise exactly as if it was a smaller resistance. After some calculation the density of current noise may be obtained in closed form

$$\frac{2\sqrt{2}KT\sqrt{\frac{\omega C}{R}}\left(\mathrm{Sin}[\sqrt{2\omega RC}]+\mathrm{Sinh}[\sqrt{2\omega RC}]\right)}{\mathrm{Cosh}[\sqrt{2\omega RC}]-\mathrm{Cos}[\sqrt{2\omega RC}]} \tag{16}$$

Now that we have the exact expression of the noise produced by the distributed-parameters device it is interesting to compare it with the results obtained with a commercial simulator, which implements a R-C chain model to describe the resistor. Since in every technology, fixed the width of the resistor, the resistance and capacitance per unit length are constants, we chose these three combinations: ($R = 10M\Omega$, $C = 1pF$), ($R = 100M\Omega$, $C = 10pF$, which reflect the device we have realized) and ($R = 1G\Omega$, $C = 100pF$). It's interesting to notice that the results are in agreement at low frequency, where the capacitive coupling is negligible. Both models show a noise corner frequency depending on R and C. At high frequency the model of the simulator suffers from its discrete nature: the maximum spectral noise density generated is the one of the single resistor in the R-C chain, while our model has a clear $\sqrt{frequency}$ behavior.

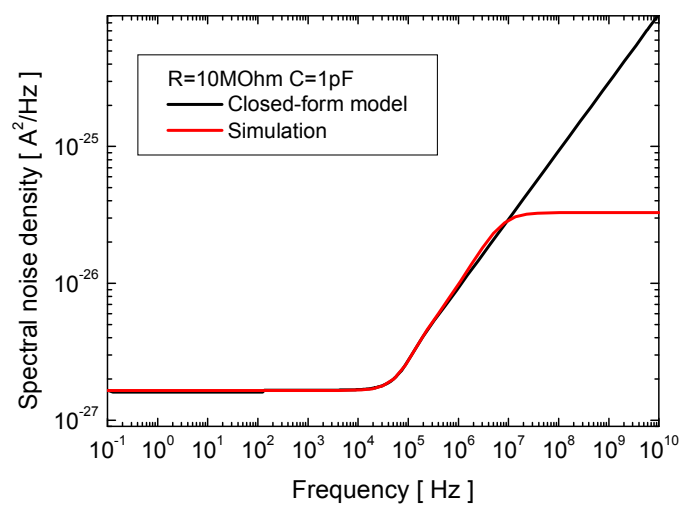

Fig. 7. Spectral noise density produced by a resistor with parameters $R = 10M\Omega$ and $C = 1pF$. Comparison between model and simulator.

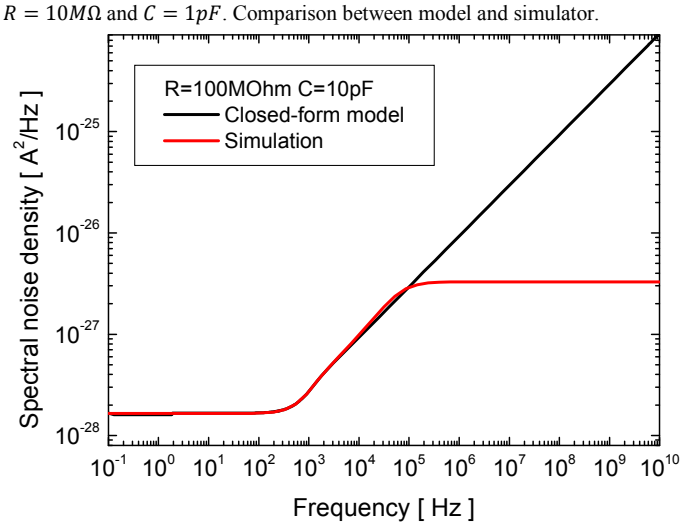

Fig. 8. Spectral noise density generated by a resistor with parameters $R = 100M\Omega$ and $C = 10pF$. Comparison between model and simulator.

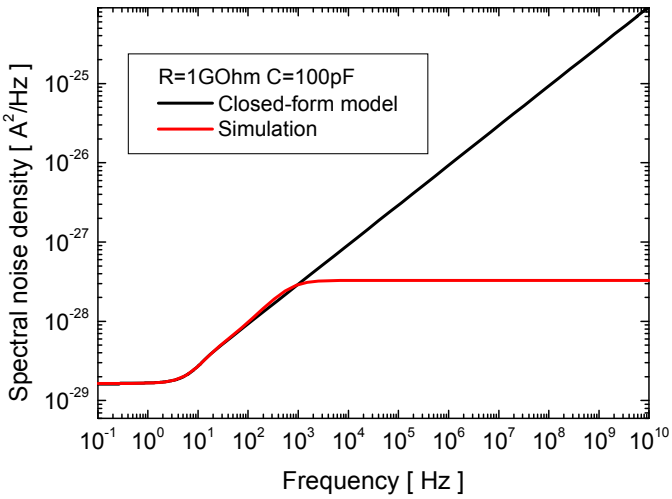

Fig. 9. Spectral noise density produced by a resistor with parameters $R = 1G\Omega$ and $C = 100pF$. Comparison between model and simulator.

The spectral noise density generated by resistors of different values are plotted in Fig. 7, 8 and 9. The rise of the noise as the square root of frequency has particular implications in the field of nuclear spectroscopy. In fact if we use such a resistor as a feedback continuous-time reset device for a charge-sensitive preamplifier, it is expected to introduce two contributions to the squared Equivalent Noise Charge: a classical one scaling with the shaping time, and a second one scaling with the square root of the shaping time. The relative weight of these contributions depends on the specific resistance and capacitance of the polysilicon layer of the device. A study on the impact to the Equivalent Noise Charge of such two contributions in typical cases will be done somewhere else.

IV. First-order correction of the impedance

Another problem which affects a charge-sensitive preamplifier with a feedback resistor characterized by a high capacitive coupling to bulk is the deformation of the shape of the output signals. In fact the impulse response of such a system should be an exponential decay whose constant is determined by the product of the feedback resistance and capacitance,

$$\frac{V_{out}}{I_{in}} = \frac{R}{1+sRC} \tag{17}$$

This fact is only true for an ideal resistor with impedance R. If that device has different impedance, like the one we can calculate from (8), then we should expect significant variations in the response function respect to (17). The effects of the parasitic capacitance are clearly visible in Fig. 9, where the deformation of the output signals due to a "transmission line" effect of the feedback net is clearly visible. This can be a problem [1] in the context of gamma spectroscopy because the shape variations of the CSP signals can spoil the resolution performance of the shaping system. Although there is no way to get rid of the additional noise due to the capacitive coupling, we can try a zero–order solution to the problem of the CSP signal deformation. The idea is based on a low-impedance (5kΩ total) voltage divider which drives a series of ten wells located under the ten parts that constitute the resistor. The two terminals of the guard must reproduce the voltages of the two terminals of the main device. This leads to a minimization of the capacitive effects affecting the resistor's behavior. Its impedance is now close to the one of a discrete component.

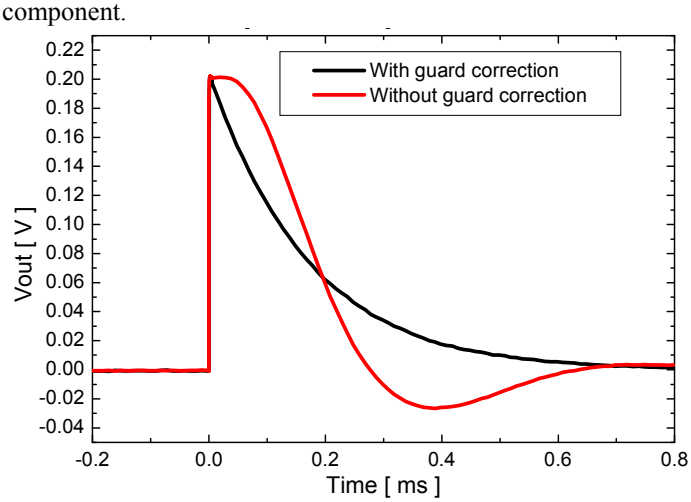

Fig. 10. Output signals from a CSP realized with a commercial discrete operational amplifier using an integrated poly-silicon 100MΩ feedback resistor characterized by 10pF of distributed parasitic capacitance. If we do not apply a correction to the potential of the 10 n-wells under the resistor it behaves like a transmission line and the ideal exponential decay response of the CSP is highly deformed. Applying the correction we obtain a waveform definitely closer to the ideal case.

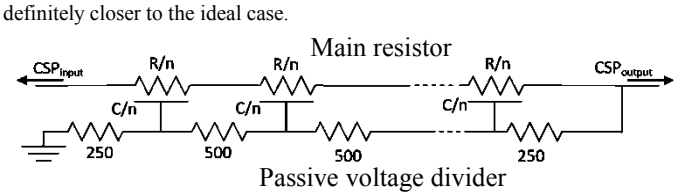

Fig. 11. Schematic diagram of the realized 100MΩ integrated resistor with low-impedance passive voltage divider which drives ten n-wells under the poly-silicon layer. In this configuration the parasitic coupling of the main resistor to bulk is minimized. The left terminal of the voltage divider is connected to ground to reproduce the voltage of the virtual ground of the input of the CSP, while the right terminal is directly connected to the low-impedance output of the preamplifier.

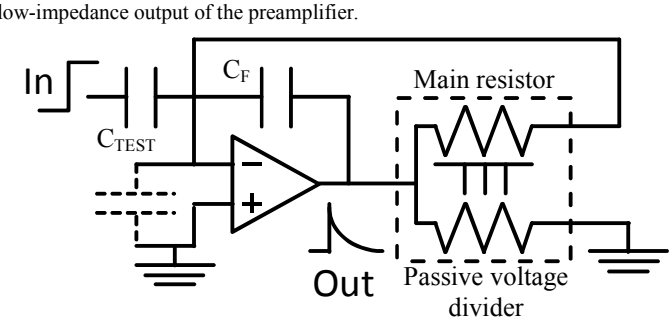

Fig. 12. Schematic diagram of the CSP with the integrated 100MΩ poly-silicon resistor as feedback discharge device. C_F is the feedback capacitor and C_{IN} is the test capacitance to simulate the charge production of the detector. The passive voltage divider which drives the n-wells under the poly-silicon layer is connected between the output node of the CSP and ground.

V. Conclusions

The implementation of the cascade of n-wells biased through a passive low-impedance voltage divider to minimize the effects of the parasitic capacitance of an integrated 100MΩ

poly-silicon resistor was experimentally found to be functional. A simple test board with a commercial operational amplifier configured in a charge-sensitive mode with our integrated device as feedback resistor demonstrated that the problems connected to the "transmission line" behavior are solved at the first order and the shape of the signals generated are clearly exponential. More advanced research, both theoretical and experimental, will be performed on the noise parameters of the system. In the near future we will connect the device to a low-noise CSP [2]-[5] in order to evaluate the impact on the Equivalent Noise Charge of our device.

REFERENCES

[1] A. Georgiev, W. Gast, R.M. Lieder, "An analog-to-digital conversion based on a moving window deconvolution", IEEE Trans. Nucl. Sci., vol. 41, no. 4, pp. 1116-1124, 1994

[2] A. Pullia, F. Zocca and S. Capra, "An Integrated Low-Noise Charge-Sensitive Preamplifier with Virtually Unlimited Spectroscopic Dynamic Range", Published in: NSS/MIC, 2012 IEEE Date of Conference: Oct. 27 2012-Nov. 3 2012 Page(s): 693 - 696 ISSN : 1082-3654 Print ISBN: 978-1-4673-2028-3

[3] A. Pullia and F. Zocca, "A low-noise preamplifier for γ-ray sensors with add-on device for large-signal management", Nucl. Instrum. and Meth., vol. A545, pp. 784–792, 2005

[4] A. Pullia et al., "An Advanced Preamplifier for Highly Segmented Germanium Detectors", IEEE Trans. Nucl. Sci., vol. 53, no. 5, pp. 2869-2875, 2006

[5] A. Pullia, G. Pascovici, C. Ur, "A versatile Low-Noise Wide-Range Charge-Sensitive Preamplifier for HPGe Detectors", IEEE Nuclear Science Symposium Conference Record, pp. 815-818, 2012, Article n. 6551217, DOI: 10.1109/NSSMIC.2012.6551217